*Journal of Photochemistry*, 6 (1976/77) 157 - 172



# THE PHOTOLYSIS OF SULFUR DIOXIDE IN THE PRESENCE OF FOREIGN GASES. VIII: EXCITATION OF $SO_2$ AT 3600 - 4100 Å IN THE PRESENCE OF ACETYLENE

NELSON KELLY, JAMES F. MEAGHER* and JULIEN HEICKLEN

*Department of Chemistry and Center for Air Environment Studies, The Pennsylvania State University, University Park, Pa 16802 (U.S.A.)*

(Received April 14, 1976)

## Summary

$SO_2$ was photolyzed at 25 °C with a band of radiation from 3600 to 4100 Å in the presence of acetylene. The quantum yield of the sole gas phase product, CO, was determined for a wide range of $SO_2$ and $C_2H_2$ pressures and in the presence of $CO_2$, NO, and $H_2O$. For all $SO_2$ pressures used, $\Phi\{CO\}$ increases with $[C_2H_2]$ to an upper limiting value of 0.190. Although the excitation corresponds mainly to the absorption $SO_2(^3B_1) \leftarrow SO_2(X, {}^1A_1)$, both the non-emitting triplet and singlet previously proposed to be important in the photochemistry of $SO_2$, as well as the emitting triplet, are necessary to interpret the results of this study. Absorption directly to a singlet state $SO_2^*$ must occur ~5% of the time. A complete mechanism, similar to that with 3130 Å, is proposed, and the pertinent rate coefficient ratios evaluated. They agree with those obtained with 3130 Å excitation.

## Introduction

Recently the photolysis of $SO_2$ in the presence of acetylene at 3130 Å to produce CO and a solid aerosol was reported from this laboratory [1, 2]. The reaction was shown to proceed solely through triplet states, both the emitting triplet, designated $SO_2(^3B_1)$ and a non-emitting triplet designated $SO_2^{**}$ [3]. The $SO_2^{**}$ was produced from two sources. At high pressures it was produced by a collisionally induced intersystem crossing from one of the singlets initially formed on absorption. There was some evidence that the $SO_2^{**}$ state was also produced by crossing induced by collision with NO from a third triplet designated $SO_2^{\dagger}$. There is evidence for these states ($SO_2^{**}$

*Present address: Tennessee Valley Authority, Air Quality Branch, Muscle Shoals, Alabama 35660 (U.S.A.).

and $SO_2^{\dagger}$) being the $^3A_2$ and $^3B_2$ states but no ordering of the energies could be made on the basis of the data. All three of the triplets are strongly quenched by NO. $CO_2$ and $H_2O$ quench the $SO_2(^3B_1)$ state but had no effect on the $SO_2^{**}$ or $SO_2^{\dagger}$ states.

It has been established that $SO_2(^3B_1)$ and $SO_2(^1B_1)$ are produced when $SO_2$ is excited into the first allowed band [4 - 16]. However, while it is generally agreed that the states initially produced on absorption are singlets, their spectroscopic designation as well as the efficiency with which $SO_2(^3B_1)$ is produced from them by intersystem crossing are still being contended. (For a discussion of the spectroscopic assignments for the excited states of $SO_2$ produced with irradiation from 2800 to 4100 Å see refs. 17 - 20.) In our previous work on the $SO_2/C_2H_2$ system the intersystem crossing ratio from the initially formed singlet to $SO_2(^3B_1)$ was assumed to be constant at 0.10. Recently higher values have been proposed for this ratio [21, 22].

It is generally agreed that the $SO_2(^3B_1)$ state is important in the reactions of excited $SO_2$. In studies with excitation into the first allowed band, the reactions of $SO_2$ in the presence of hydrocarbons and CO were ascribed to $SO_2(^3B_1)$ [21, 23 - 26]. Further proof of the reactivity of this state was given by directly exciting the $SO_2(^3B_1) \leftarrow SO_2(X, {}^1A_1)$ forbidden band of $SO_2$ [27 - 32]. Jackson and Calvert [27] worked at high pressures in their study of the photo-oxidation of CO by $SO_2$ excited at 3600 - 4100 Å and were able to explain their product yields of $CO_2$ as coming entirely from the $SO_2(^3B_1)$ state. However, they varied the ratio $[SO_2]/[CO]$ only over a small range. Demerjian *et al.* [29], on the other hand, in their study of the *cis–trans* isomerization of butene-2 by $SO_2$ excited at 3600 - 4100 Å varied the ratio $[SO_2]/[\text{butene-2}]$ over a wide range, and worked at both high and low pressures. They could also explain their results with only the $SO_2(^3B_1)$ state. In the study by Wampler and Bottenheim [30] of the photosensitized isomerization of 1,2-dichloroethylene by $SO_2$ irradiated at 3712 Å, it is especially convincing that the phosphorescing state is the state responsible for the chemistry. The decay of phosphorescence was followed as well as the initial rate of production of products. Within the experimental error Wampler and Bottenheim [30] obtained agreement in the quenching rate constants determined from both sets of experiments.

Thus although there is extensive evidence that the $SO_2(^3B_1)$ state is reactive there are cases where this state is not important or where singlet states are the reactive states [2, 3, 33 - 37]. Also, other studies have shown that the non-emitting triplet, $SO_2^{**}$, or some other state that produces an excess of the $SO_2(^3B_1)$ state at high pressures, must be included in the mechanism [2, 21, 24, 34 - 39]. Therefore although in the $SO_2/C_2H_2$ system, $SO_2(^3B_1)$ reactivity was consistent with the low-pressure results, it is still important to investigate its reactivity directly.

Direct absorption into the $SO_2(^3B_1)$ state should allow us to study the reactivity of this state without the complications of intersystem crossing. Moreover, this system is ideal for the study of the photolysis of high pressures of $SO_2$ which could not be done with irradiation at 3130 Å. Also, it

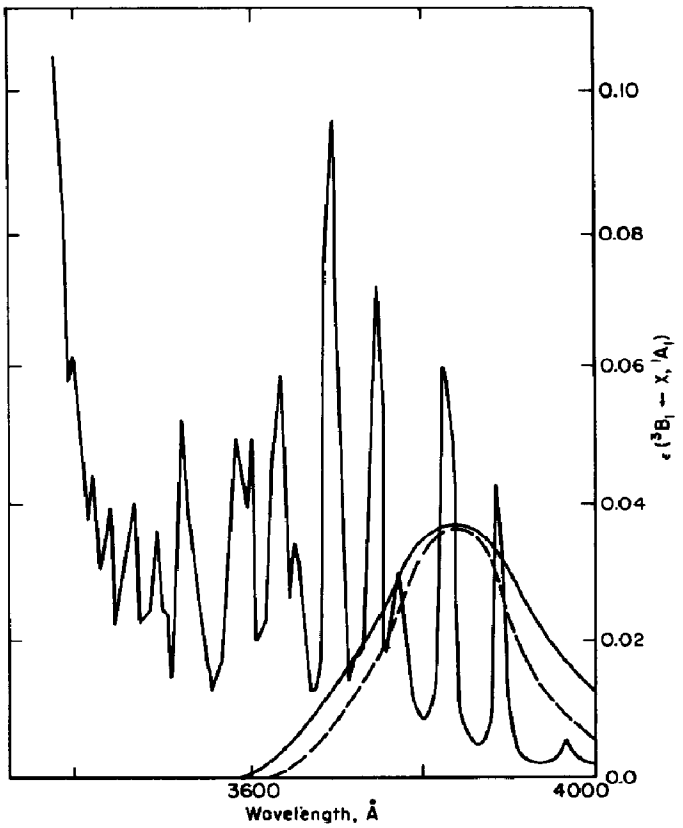


Fig. 1. Absorption spectrum of $SO_2$ (from Chung *et al.* [39]). —— (In lower right-hand corner), spectral band of the incident radiation used in this study; - - - -, incident radiation of Chung *et al.* [39].

might be possible to see if $SO_2(^3B_1)$ is quenched to some other triplet, which has been proposed recently [40]. The systems in which more than just the optical states $SO_2(^1B_1)$ and $SO_2(^3B_1)$ are needed to rationalize the results all seem to be high pressure systems. In order to investigate these features of $SO_2$ photochemistry we have undertaken the photolysis of $SO_2$ with radiation centered about 3850 Å in the presence of acetylene and various other quenching gases.

## Experimental

The apparatus used in this study is, with a few exceptions, the same as that described in our earlier paper [3]. The gas handling and purification procedures are exactly as described before. Two photolysis cells were used in this study. Some data were taken in the original cell (50 cm × 5 cm o.d. cylindrical cell) used in the previous study but a 1.5 m cell was used for the bulk of the measurements.

The radiation source was a 150 W d.c. high pressure xenon arc lamp (Hanovia model 901-C1). The light was collimated by a quartz lens and

passed through a piece of flint glass, a Corning 7-54 (9863) glass filter, and an Oreil G-772-3900 Long Pass filter. A monochromator was placed at the back of the cell and a phototube was used to measure the radiation passing through the cell. The spectral distribution is shown in Fig. 1, superimposed on the absorption spectrum of $SO_2$. The full-width half-maximum (FWHM) of the incident radiation band is 230 Å.

In order to measure the absorbed intensity it was necessary to match the absorbance of $SO_2$ in this band to that of azomethane, which has a quantum yield of nitrogen production equal to 1.0 [41]. This was done in two ways.

First, the average decadic extinction coefficient was determined absolutely by measuring the change in intensity as $SO_2$ was added to the cell. A plot of absorbance *vs.* $SO_2$ pressure yielded a straight line. The value obtained in this way was $\overline{\epsilon_{10}} = 0.0119 \pm 0.0023$ l/mol cm. Using a band of radiation similar to ours, Demerjian *et al.* [29] obtained $\overline{\epsilon_{10}} = 0.0266 \pm 0.0064$ l/mol cm while Wampler and Bottenheim [30] obtained $\overline{\epsilon_{10}} = 0.027 \pm 0.002$ l/mol cm. The discrepancy between our results and theirs can be attributed to more longer wavelength light in our band where the extinction coefficient of $SO_2$ is diminishing.

The second method of determining the extinction coefficient was an indirect one. The extinction coefficient of azomethane was determined by measuring the absorbance for 2 to 50 Torr azomethane pressures. The azomethane absorbance was then very carefully matched to $SO_2$ absorbance over a range of pressures and a constant of proportionality was determined for their extinction coefficients. It took 105 times as much $SO_2$ to absorb the same amount of light as a given pressure of azomethane. From this factor and the extinction coefficient of azomethane the extinction coefficient of $SO_2$ was found to be $\overline{\epsilon_{10}} = 0.0106 \pm 0.0010$ l/mol cm. It is interesting that no pressure broadening was seen in any of these experiments.

The same analytical procedure was used to collect and measure CO and $N_2$ as was previously described [3]. However, to increase reproducibility, a small amount of He was added to the cell after each run to aid in transporting the CO to the gas chromatograph. Photolysis times were kept as short as possible so that the concentrations of reactants remained virtually constant and initial quantum yields were measured.

## Results

All experiments were carried out at 25 °C. First, it was verified that $SO_2$ excited with a band from 3600 to 4100 Å reacts with acetylene to produce CO. Once this was established carbon monoxide analyses for identical experiments with a $SO_2$ pressure of 25 Torr and a $C_2H_2$ pressure of 12.1 Torr for a variety of exposure times were performed. It was found that the CO growth was linear and showed no detectable induction period or fall-off at longer exposures. This indicates that CO is an initial product and that there is not a

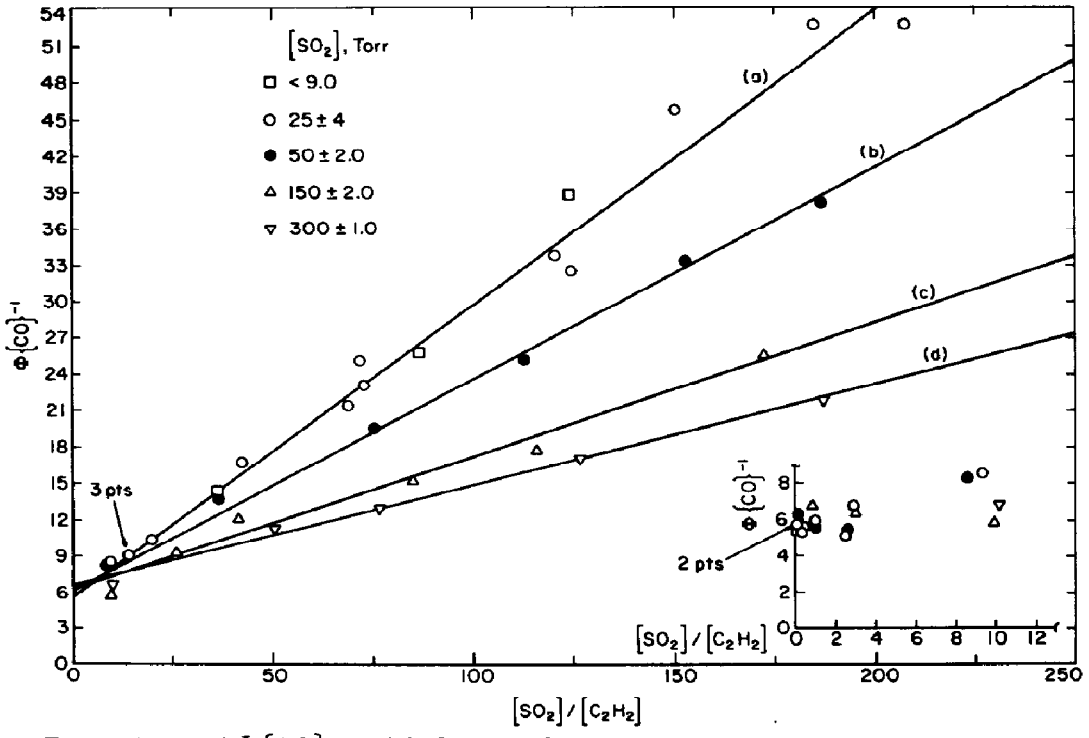


Fig. 2. Plots of $\Phi\{CO\}$ *vs.* $[SO_2]/[C_2H_2]$ for various $SO_2$ pressures. Curves (a), (b), (c) and (d) are for ≤ 25, 50, 150 and 300 Torr of $SO_2$ respectively.

significant amount of light scattering from the aerosol under the conditions we have employed.

With the $SO_2$ pressure at 25 ± 2.0 Torr and the absorbed intensity $I_a$ between 0.012 and 0.039 mTorr/min, the $C_2H_2$ pressure was varied from 120 mTorr to 260 Torr. A number of runs also were done with $SO_2$ pressures less than 25 Torr. The reciprocal CO quantum yields, $\Phi\{CO\}^{-1}$ for these runs vary linearly with $[SO_2]/[C_2H_2]$ as shown in Fig. 2, curve (a).

Three series of runs were done at higher pressures of $SO_2$: $[SO_2]$ = 50 ± 2.0 Torr, $I_a$ = 0.076 mTorr/min, and $[C_2H_2]$ = 0.259 - 301 Torr; $[SO_2]$ = 150 ± 2.0 Torr, $I_a$ = 0.22 mTorr/min, and $[C_2H_2]$ = 0.866 — 155 Torr; and $[SO_2]$ = 300 ± 1 Torr, $I_a$ = 0.44 mTorr/min; and $[C_2H_2]$ = 1.61 — 29.8 Torr. For each of these series, $\Phi\{CO\}^{-1}$ varies linearly with $[SO_2]/[C_2H_2]$, as shown in Fig. 2, but the lines lie successively lower as the $SO_2$ pressure is raised.

Experiments were done with a $SO_2$ pressure of 25 ± 1 Torr, $I_a$ = (13.5 ± 0.5) × $10^{-3}$ mTorr/min, and a $C_2H_2$ pressure of 1.80 ± 0.11 Torr with $CO_2$ added up to 533 Torr. Figure 3, curve (a) shows a plot of $\Phi\{CO\}^{-1}$ *vs.* $[CO_2]$. At a $SO_2$ pressure of 6.80 ± 0.20 Torr, $I_a$ = (3.57 ± 0.06) × $10^{-3}$ mTorr/min, and a $C_2H_2$ pressure of 1.81 ± 0.01 Torr, $CO_2$ was added up to 691 Torr. Figure 3, curve (b) shows a plot of $\Phi\{CO\}^{-1}$ *vs.* $[CO_2]$ for these data. In each of these series $\Phi\{CO\}^{-1}$ varies linearly with $[CO_2]$, the line at higher $SO_2$ pressure lying above that at lower $SO_2$ pressure.

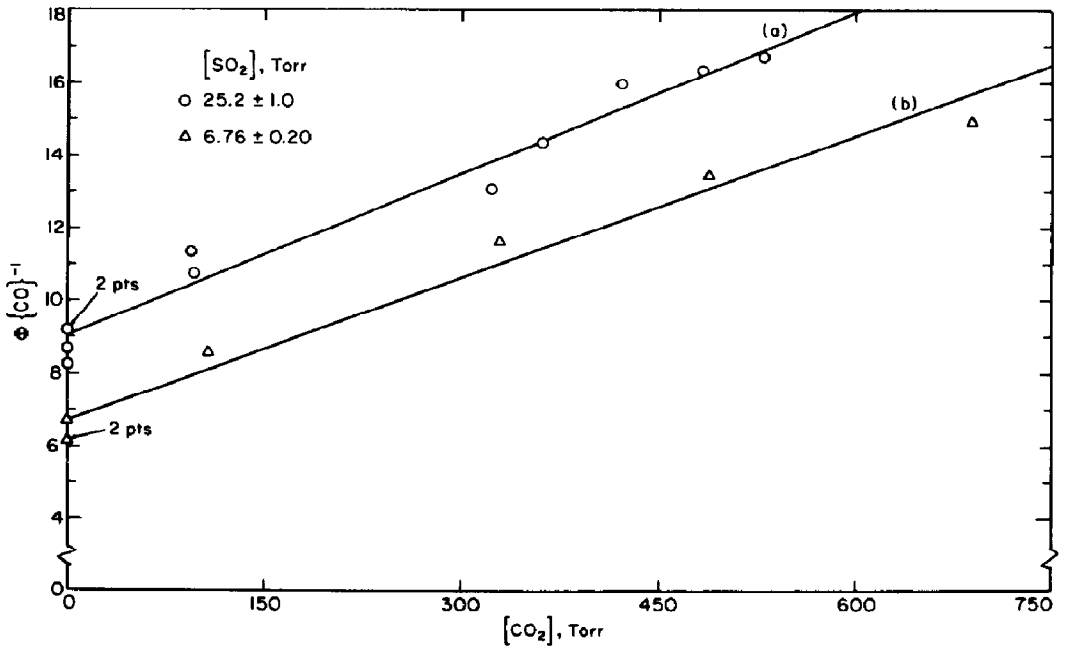


Fig. 3. Plots of $\Phi\{CO\}^{-1}$ *vs.* $[CO_2]$. (a) $[SO_2] = 25.2 \pm 1.0$, $[C_2H_2] = 1.80 \pm 0.11$ Torr; (b) $[SO_2] = 6.76 \pm 0.20$, $[C_2H_2] = 1.81 \pm 0.01$ Torr.

Another series of runs with a $SO_2$ pressure of 25 ± 1.0 Torr, $I_a$ = (13.3 ± 0.5) × $10^{-3}$ mTorr/min, and $C_2H_2$ pressure of 2.71 ± 0.10 Torr was done with NO as the quenching gas. Figure 4 shows a plot of $\Phi\{CO\}^{-1}$ *vs.* [NO], and this plot is also linear.

A few runs were also done at 25 Torr of $SO_2$, 1.81 Torr of $C_2H_2$ and $I_a$ = (13.5 ± 0.5) × $10^{-3}$ mTorr/min with water added as the quenching gas. There is a slight decrease in $\Phi\{CO\}$ with increasing $H_2O$ pressure, but this decrease is within the experimental scatter. With the same $SO_2$ pressure but with $I_a$ = (28 ± 2) × $10^{-3}$ mTorr/min and an acetylene pressure of 0.334 Torr, more runs were done with water as the quenching gas. Again $\Phi\{CO\}$ only decreased slightly and within the experimental scatter could have been constant. These runs are shown in Fig. 5.

Blank runs were done with large pressures of each of the gases to make sure there was no background CO. Also 600 Torr of $C_2H_2$ alone was irradiated for 2 h and no CO was produced. This same experiment was repeated for $SO_2$ alone, and no CO was found. In addition, a mixture of 300 Torr of $C_2H_2$ and 300 Torr of $SO_2$ were allowed to stand overnight. No dark reaction to produce CO was observed.

## Discussion

The major conclusions that can be drawn from this study are:

(1) $SO_2$ photoexcited at 3600 - 4100 Å reacts with $C_2H_2$ to produce CO.

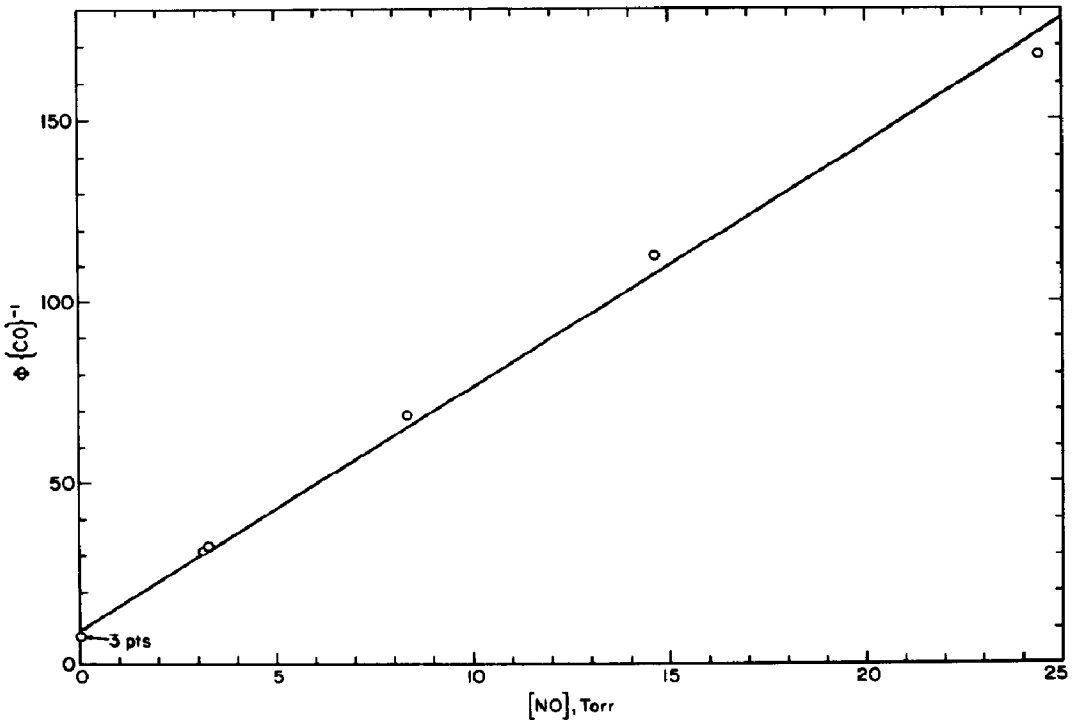


Fig. 4. Plot of $\Phi\{CO\}^{-1}$ *vs.* $[NO]$. $[SO_2] = 25.4 \pm 1.0$; $[C_2H_2] = 2.68 \pm 0.05$ Torr.

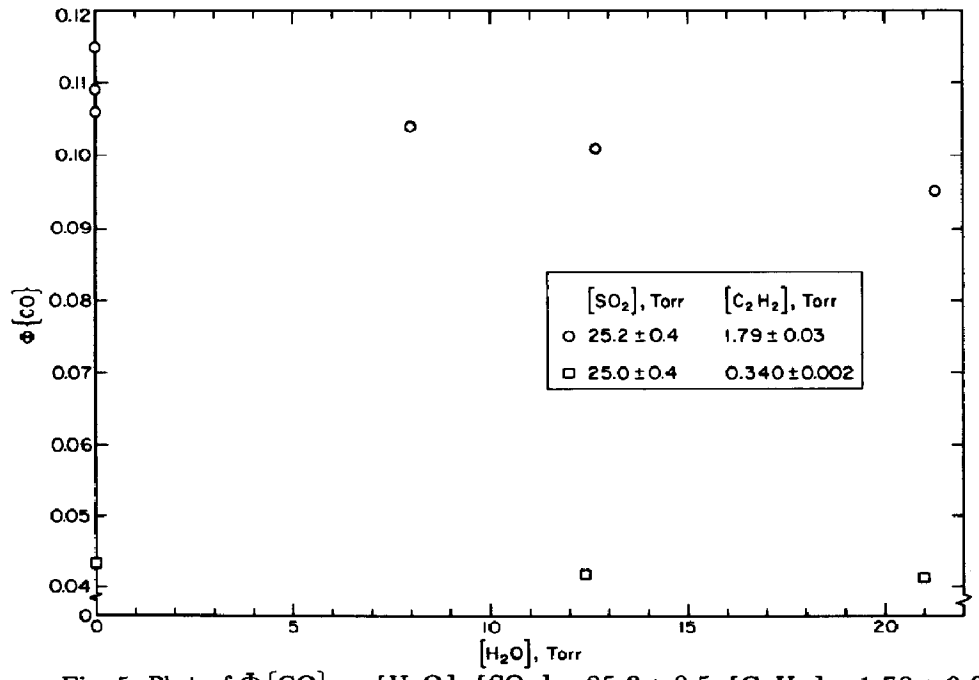


Fig. 5. Plot of $\Phi\{CO\}$ *vs.* $[H_2O]$. $[SO_2] = 25.2 \pm 0.5$, $[C_2H_2] = 1.79 \pm 0.04$ Torr.

(2) The chemically reactive states are triplets, since CO production is readily eliminated in the presence of relatively small amounts of NO, a known efficient triplet quencher.

(3) Below 25 Torr of $SO_2$, the exclusive triplet state involved is the $^3B_1$ state, because $\Phi\{CO\}$ depends only on $[SO_2]/[C_2H_2]$ in accordance with our previous information on this state. The other chemically reactive triplet, $SO_2^{**}$, which is not quenched by $SO_2$ cannot be present at low pressures.

(4) At higher $SO_2$ pressures, another state (presumably $SO_2^{**}$) contributes to CO production, since the excess contribution to $\Phi\{CO\}$ is not dependent exclusively on the ratio $[SO_2]/[C_2H_2]$.

The mechanism we have used to fit our results is similar to the one used in the 3130 Å system [3], except now $SO_2^*$ is produced at some fraction, $\beta$, of the absorbed intensity, $I_a$. The entire mechanism is:

| | | | |
|---|---|---|---|
| $SO_2 + h\nu$ | $\rightarrow {}^3SO_2$ | Rate = $(1-\beta)I_a$ | |
| | $\rightarrow SO_2^*$ | Rate = $\beta I_a$ | |
| $^3SO_2 + C_2H_2$ | $\rightarrow$ CO | | (7a) |
| | $\rightarrow$ removal | | (7b) |
| $^3SO_2 + SO_2$ | $\rightarrow$ removal | | (8a) |
| $+ CO_2$ | $\rightarrow$ removal | | (8b) |
| $+ NO$ | $\rightarrow$ removal | | (8c) |
| $+ H_2O$ | $\rightarrow$ removal | | (8d) |
| $SO_2^*$ | $\rightarrow$ removal | | (2) |
| $SO_2^* + M$ | $\rightarrow SO_2^{**} + M$ | | (3a) |
| | $\rightarrow$ removal | | (3b) |
| $SO_2^{**} + C_2H_2$ | $\rightarrow$ CO | | (9) |
| $SO_2^{**} + NO$ | $\rightarrow$ removal | | (10) |
| $SO_2^{**}$ | $\rightarrow SO_2$ | | (11) |

For comparison purposes we have used the same reaction numbers as in our previous paper [3]. Here $^3SO_2$ stands for $SO_2(^3B_1)$ the emitting triplet, which is also formed directly on absorption. The $SO_2^{**}$ state is the non-emitting triplet which is not quenched by $SO_2$ but leads to CO formation at least part of the time by reaction with $C_2H_2$. We do not have sufficient information to establish whether or not there is a physical quenching process with $C_2H_2$ and for simplicity this step is omitted.

The $SO_2^*$ state is a singlet and is produced upon absorption, *i.e.* the singlet state absorption overlaps slightly with that of the triplet and although most of the 3500 - 4100 Å band of $SO_2$ is due to the formation of triplet state there is still some singlet production left.

The mechanism predicts that:

$$\Phi\{CO\} = \frac{(1-\beta)k_{7a}[C_2H_2]}{k_7[C_2H_2] + k_8[X]} + \frac{\beta k_{3a}[M]k_9[C_2H_2]}{(k_2 + k_3[M])(k_9[C_2H_2] + k_{10}[NO] + k_{11})} \quad (I)$$

In the first term on the right-hand side of eqn. (I), [X] is $SO_2$, $CO_2$, NO, and presumably water although in this study quenching by water was not measureable. In the second term, [M] is any gas that causes the intersystem crossing of $SO_2^*$ to $SO_2^{**}$. The first term on the right-hand side is the contribution from the emitting triplet and is always the dominant term. We shall call this $\Phi^3\{CO\}$. The second term is the contribution from $SO_2^{**}$ and shall be called $\Phi^{**}\{CO\}$.

At low [M], $\Phi^3\{CO\}$ determines $\Phi\{CO\}$ and thus $\Phi\{CO\}^{-1}$ varies linearly with $[SO_2]/[C_2H_2]$. With runs where the $SO_2$ pressure is less than 25 Torr a plot of $\Phi\{CO\}^{-1}$ *vs.* $[SO_2]/[C_2H_2]$ allows us to evaluate $k_7/k_{8a}$. From Fig. 2, curve (a), the ratio of intercept to slope gives $k_7/k_{8a} = 23.5$. From the previous work at 3130 Å [3], this number was determined to be 23.0. Also $k_{7a}/k_7$ was determined before to be 0.189. This agrees well with $k_{7a}/k_7 = 0.177$ obtained in this study if $\beta$ is a small number such that $1 - \beta \sim 1$. These results are summarized in Table 1.

At higher $SO_2$ pressures Fig. 2, curves (b), (c) and (d) show that there is excess CO over that predicted by $\Phi^3\{CO\}$. Since we have determined $\Phi^3\{CO\}$ we may subtract this from $\Phi\{CO\}$ to obtain $\Phi^{**}\{CO\}$:

$$\Phi^{**}\{CO\} = \Phi\{CO\} - \Phi^3\{CO\} = \frac{\beta k_{3a}[M]k_9[C_2H_2]}{(k_2 + k_3[M])(k_9[C_2H_2] + k_{10}[NO] + k_{11})} \quad (II)$$

For the runs with NO absent and with $[SO_2] = 150$ or 300 Torr and $[C_2H_2] < 1$ Torr we approximate this as:

$$\Phi^{**}\{CO\} = \frac{\beta k_{3a}[SO_2]}{(k_2 + k_3[SO_2])} \times \frac{k_9[C_2H_2]}{(k_9[C_2H_2] + k_{11})} \quad (III)$$

Thus a plot of $\Phi^{**}\{CO\}^{-1}$ *vs.* $1/[C_2H_2]$ at constant $SO_2$ pressures of 150 or 300 Torr allows us to evaluate $k_{11}/k_9$ from the ratio of slope to intercept.

In order to smooth the data, the values of $\Phi\{CO\}$ and $\Phi^3\{CO\}$ used to calculate $\Phi^{**}\{CO\}$ were obtained from the straight lines drawn through the points of Fig. 2, curves (a), (c) and (d). Thus $\Phi^{**}\{CO\}$ for $SO_2$ pressures of 150 and 300 Torr were calculated for $[SO_2]/[C_2H_2]$ ratios of 50, 100, 150, 200, and 250 by taking the reciprocals of the values for $\Phi\{CO\}^{-1}$ in Fig. 2, curves (c) and (d). Table 2 lists the values of $\Phi^{**}\{CO\}$. In Fig. 6 are shown the plots of $\Phi^{**}\{CO\}^{-1}$ *vs.* $1/[C_2H_2]$ for the two $SO_2$ pressures of 150 and 300 Torr. The ratio of slope to intercept for $[SO_2] = 300$ and 150 Torr plots are 1.41 and 1.04 Torr respectively. A simple average gives $k_{11}/k_9 = 1.22$ Torr in good agreement with the value of 1.38 found earlier [3].

TABLE 1

Summary of rate coefficient information

| Ratio | Value | Units | M | Reference |
|---|---|---|---|---|
| $k_{7a}/k_7$ | 0.177 | None | $C_2H_2$ | This work |
| | 0.189 | None | $C_2H_2$ | Kelly *et al.* [3] |
| $k_7/k_{8a}$ | 23.5 | None | $C_2H_2$ | This work |
| | 23.0 | None | $C_2H_2$ | Kelly *et al.* [3] |
| $k_{8b}/k_{8a}$ | 0.42 | None | $CO_2$ | Kelly *et al.* [3] |
| | 0.31 | None | $CO_2$ | Mettee [9] |
| | 0.29 | None | $CO_2$ | Sidebottom *et al.* [42] |
| | 0.55 | None | $CO_2$ | Stockburger *et al.* [16] |
| $k_{8c}/k_{8a}$ | 74.4 | None | NO | This work |
| | 80.0 | None | NO | Kelly *et al.* [3] |
| | 64.0 | None | NO | Mettee [9] |
| | 100 | None | NO | Stockburger *et al.* [16] |
| | 190 | None | NO | Sidebottom *et al.* [42] |
| | 200 | None | NO | Penzhorn and Gusten [25] |
| $k_{11}/k_9$ | 1.22 | Torr | $C_2H_2$ | This work |
| | 1.38 | Torr | $C_2H_2$ | Kelly *et al.* [3] |
| $k_2/k_3$ | 70.6 | Torr | $CO_2$ | This work |
| | 56.0 | Torr | $CO_2$ | Kelly *et al.* [3] |
| | 32.7 | Torr | $H_2O$ | This work |
| | 4.41 | Torr | $H_2O$ | Kelly *et al.* [3] |
| | ~10 | Torr | $H_2O$ | Stockburger *et al.* [16] |
| | ~32 | Torr | $SO_2$ | This work |
| $k_{3a}/k_3$ | ~1 | None | $SO_2$ | This work |
| $\beta$ | $\geq 0.05$ | None | — | This work |

This value for $k_{11}/k_9$ can be used along with $\Phi^{**}\{CO\}$ listed in Table 2 to calculate $\Phi^{**}\{CO\}(1 + 1.22\ \text{Torr}/[C_2H_2])$. Table 3 shows the value of this function for different $[SO_2]/[C_2H_2]$ ratios and for $SO_2$ pressures of 50, 150, and 300 Torr. It is also shown for 25 Torr of $SO_2$ but this will be

TABLE 2

Average quantum yields

| $[SO_2]$ | $\Phi\{CO\}$ | | | | $\Phi^{**}\{CO\}^a$ | | |
|---|---|---|---|---|---|---|---|
| $[C_2H_2]$ | $[SO_2] = 300$ Torr | $[SO_2] = 150$ Torr | $[SO_2] = 50$ Torr | $[SO_2] < 25$ Torr | $[SO_2] = 300$ Torr | $[SO_2] = 150$ Torr | $[SO_2] = 50$ Torr |
| 50 | 0.0934 | 0.0854 | 0.0680 | 0.0570 | 0.0364 | 0.0284 | 0.011 |
| 100 | 0.0677 | 0.0585 | 0.0426 | 0.0338 | 0.0339 | 0.0247 | 0.0088 |
| 150 | 0.0529 | 0.0441 | 0.0310 | 0.0241 | 0.0288 | 0.0200 | 0.0069 |
| 200 | 0.0433 | 0.0355 | 0.0244 | 0.0186 | 0.0247 | 0.0169 | 0.0058 |
| 250 | 0.0366 | 0.0297 | 0.0201 | 0.0152 | 0.0214 | 0.0145 | 0.0049 |

[a]Computed as $\Phi\{CO\} - \Phi^3\{CO\}$ where $\Phi^3\{CO\}$ is $\Phi\{CO\}$ for $[SO_2] < 25$ Torr.

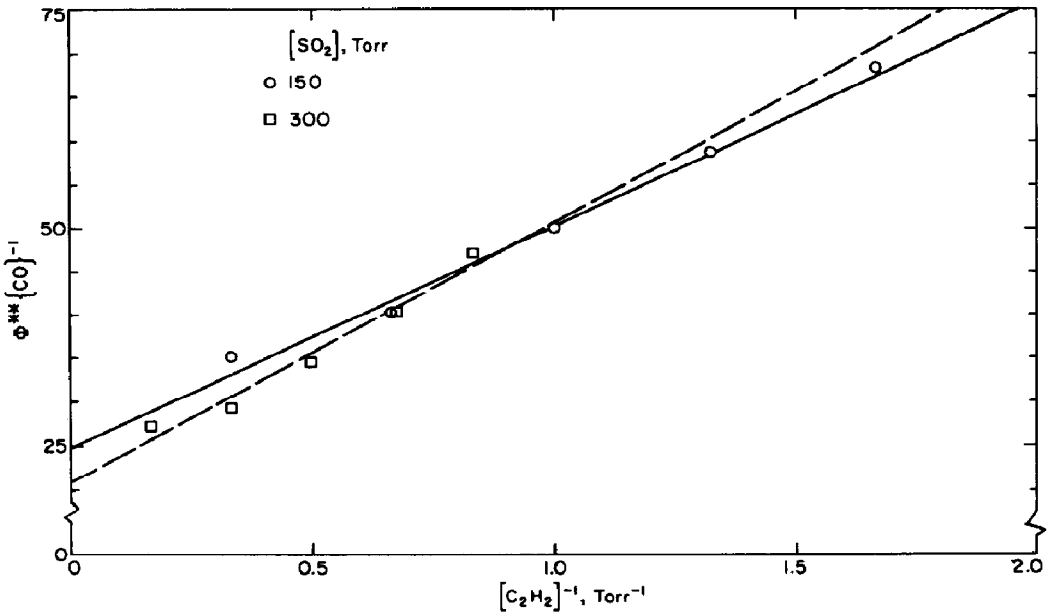


Fig. 6. Plots of $\Phi^{**}\{CO\}^{-1}$ *vs.* $1/[C_2H_2]$. The points on this curve are not data points but are the average values listed in Table 2.

explained later since $\Phi\{CO\}$ and $\Phi^3\{CO\}$ were assumed to be the same at 25 Torr of $SO_2$. The function should be independent of $[SO_2]/[C_2H_2]$ at each $SO_2$ pressure. Except for one low value at $[SO_2]/[C_2H_2] = 50$ and $[SO_2] = 50$ Torr, it is constant at 0.0452 ± 0.0038, 0.0436 ± 0.0042 and 0.0312 ± 0.0042 for $SO_2$ pressures of 300, 150, and 50 Torr respectively.

Equation (III) can be rearranged to give:

$$\Phi^{**}\{CO\}^{-1}\,(1 + 1.22\ \text{Torr}/[C_2H_2])^{-1} = (k_3/\beta k_{3a})(1 + k_2/k_3\,[SO_2]) \quad \text{(IV)}$$

If we plot $\Phi^{**}\{CO\}^{-1}\,(1 + 1.22\ \text{Torr}/[C_2H_2])^{-1}$ *vs.* $[SO_2]^{-1}$ for the three $SO_2$ pressures above 25 Torr we may estimate $k_2/k_3$ for $SO_2$ as M. Figure 7 is such a plot. The intercept gives $k_3/\beta k_{3a} = 19.5$. Since $\beta \ll 1$, we may assume $k_{3a}/k_3 \simeq 1$, which gives a lower limiting value for $\beta \simeq 0.05$. From the ratio of slope to intercept (Fig. 7) we obtain $k_2/k_3 = 32$ Torr. In the study of

TABLE 3

Values of $\Phi^{**}\{CO\}\,(1 + 1.22\ \text{Torr}/[C_2H_2])$ for various conditions

| $[SO_2]/[C_2H_2]$ | $\Phi^{**}\{CO\}\,(1 + 1.22\ \text{Torr}/[C_2H_2])$ | | | |
|---|---|---|---|---|
| | $[SO_2] = 300$ Torr | $[SO_2] = 150$ Torr | $[SO_2] = 50$ Torr | $[SO_2] = 25$ Torr |
| 50 | 0.0438 | 0.0399 | 0.0244 | 0.00655 |
| 100 | 0.0477 | 0.0448 | 0.0302 | 0.00384 |
| 150 | 0.0465 | 0.0446 | 0.0324 | 0.00269 |
| 200 | 0.0447 | 0.0444 | 0.0340 | 0.00210 |
| 250 | 0.0431 | 0.0443 | 0.0348 | 0.00169 |

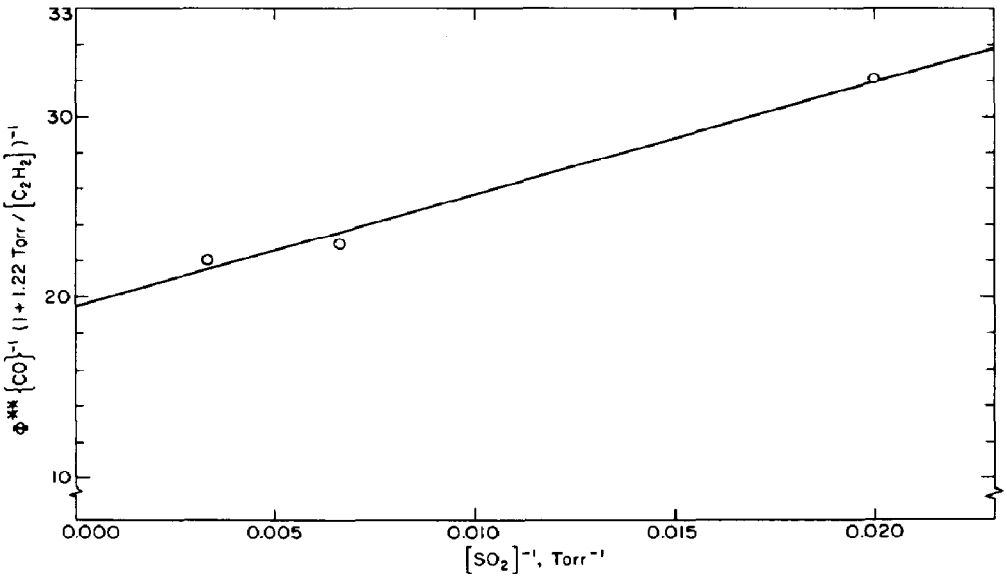


Fig. 7. Plots of $\Phi^{**}\{CO\}^{-1}$ (1 + 1.22 Torr/$[C_2H_2]$)$^{-1}$ *vs.* 1/$[SO_2]$. The function $\Phi^{**}\{CO\}^{-1}$ (1 + 1.22 Torr/$[C_2H_2]$)$^{-1}$ is the average value at each of the three $SO_2$ pressures of 50, 150 and 300 Torr listed in Table 3.

this system at 3130 Å reaction (3) was not included in the mechanism because there the $SO_2$ pressure never exceeded 20 Torr, and the effect of reaction (3) was not apparent.

Using the slope and intercept of Fig. 7 we may obtain the function $\Phi^{**}\{CO\}$ (1 + 1.22 Torr/$[C_2H_2]$) for $[SO_2]$ = 25 Torr. It is seen that this is very small in comparison to the values at $[SO_2]$ = 150 and 300 Torr and it is not constant. This is because at $[SO_2]$ = 25 Torr, $\Phi^{**}\{CO\}$ is really negligible and for all practical purposes $\Phi\{CO\} = \Phi^{3}\{CO\}$, as we have assumed. However, since $\Phi^{**}\{CO\}$ at 25 Torr is anywhere from 30 to 50% of $\Phi^{**}\{CO\}$ at 50 Torr there would be a large error in using $\Phi^{**}\{CO\}$ *vs.* 1/$[C_2H_2]$ at $[SO_2]$ = 50 Torr to get $k_{11}/k_9$ while at $[SO_2]$ = 150 or 300 Torr this is not the case. Thus even though there is some CO produced from $SO_2^{**}$ at 25 Torr the effect is nearly negligible and was not needed by any previous workers to explain the photoreactions of $SO_2$ excited in the first allowed band. The large uncertainty in $\Phi^{**}\{CO\}$ at 50 Torr also introduces a very large uncertainty in $k_2/k_3$, and this value could be in error by a factor of 2.

With $CO_2$ added we are unable to uncouple contributions of $\Phi^{3}\{CO\}$ and $\Phi^{**}\{CO\}$. This is because $SO_2^{*}$ is crossing to $SO_2^{**}$ by $CO_2$ quenching when quenching of $SO_2(^3B_1)$ by $CO_2$ becomes noticeable. However, if we use the rate constant ratio, $k_{8b}/k_{8a}$, obtained at low pressures in the previous study [3], we may evaluate $\Phi^{3}\{CO\}$ and subtract it from $\Phi\{CO\}$ to obtain $\Phi^{**}\{CO\}$. Again to smooth the data we evaluate $\Phi\{CO\}$ from the best line drawn through the points in Fig. 3. This is done because the experimental accuracy is such that it is hard to see any difference in $\Phi\{CO\}$ for runs at 50 or 100 Torr of $CO_2$. Yet the lines drawn in Fig. 3 allow us to get a trend

TABLE 4

Average quantum yields in the presence of $CO_2$

| $[CO_2]$ (Torr) | $\Phi\{CO\}^a$ | $\Phi^3\{CO\}^b$ | $\Phi^{**}\{CO\}^c$ |
|---|---|---|---|
| | $[SO_2]$ = 25.2 Torr, $[C_2H_2]$ = 1.80 Torr | | |
| 50 | 0.1025 | 0.0849 | 0.0176 |
| 75 | 0.0988 | 0.0759 | 0.0229 |
| 100 | 0.0952 | 0.0687 | 0.0265 |
| 200 | 0.0833 | 0.0497 | 0.0336 |
| 300 | 0.0769 | 0.0389 | 0.0380 |
| 400 | 0.0669 | 0.0320 | 0.0350 |
| | $[SO_2]$ = 6.76 Torr, $[C_2H_2]$ = 1.81 Torr | | |
| 50 | 0.1350 | 0.109 | 0.0260 |
| 75 | 0.1300 | 0.0950 | 0.0350 |
| 100 | 0.125 | 0.0837 | 0.0413 |
| 200 | 0.107 | 0.0571 | 0.0499 |
| 300 | 0.0942 | 0.0434 | 0.0508 |
| 400 | 0.0840 | 0.0349 | 0.0491 |

[a]From lines in Fig. 3. [b]From eqn. (V). [c]Calculated as $\Phi\{CO\} - \Phi^3\{CO\}$.

between large pressure differences of $CO_2$ such that we can estimate differences in $\Phi\{CO\}$ between pressures of 50 and 100 Torr of $CO_2$. In Table 4 are listed values of $\Phi\{CO\}$ and $\Phi^3\{CO\}$ obtained from Fig. 3 and using the expression:

$$\Phi^3\{CO\} = \frac{k_{7a}[C_2H_2]}{k_7[C_2H_2] + k_{8a}[SO_2] + k_{8b}[CO_2]} \qquad (V)$$

The ratio $k_{8b}/k_{8a} = 0.42$ [3] was used in evaluating this expression.

Since now $CO_2$ is the M gas in reaction (3), the expression relating $\Phi^{**}\{CO\}$ to the mechanism is:

$$\Phi^{**}\{CO\}^{-1} = (1 + k_{11}/k_9[C_2H_2])(k_3/k_{3a}\beta)(1 + k_2/k_3[CO_2]) \qquad (VI)$$

We may plot $\Phi^{**}\{CO\}^{-1}$ obtained using the numbers in Table 4 *vs.* $1/[CO_2]$. At high $CO_2$ pressures we see that $\Phi^{**}\{CO\}$ drops which suggests that there is a slight quenching of $SO_2^{**}$ by $CO_2$, which we have neglected. Ignoring this effect, we evaluate $k_2/k_3$ from the slopes and intercepts of Fig. 8 for the two $SO_2$ pressures. We obtain 76.8 and 64.5 Torr for $k_2/k_3$ for $[SO_2]$ = 25.2 and 6.8 Torr, respectively. The average is 70.6 Torr. In the study at 3130 Å the value obtained for $k_2/k_3$ was 56 Torr for $CO_2$ as [M] in reaction (3). However, it must be remembered that the $SO_2^*$ produced here has much different vibrational excitation than $SO_2^*$ produced at a different wavelength, and the rate coefficient ratios need not necessarily be the same.

The intercepts of the lines in Fig. 8 when coupled with $k_{11}/k_9 = 1.22$ Torr give $k_3/k_{3a}\beta = 13$ and 10, respectively, for $[SO_2]$ = 25.2 and 6.76 Torr. These values are somewhat lower than 19.5 found in the absence of $CO_2$, but considering the errors involved can be considered to be in reasonable agreement.

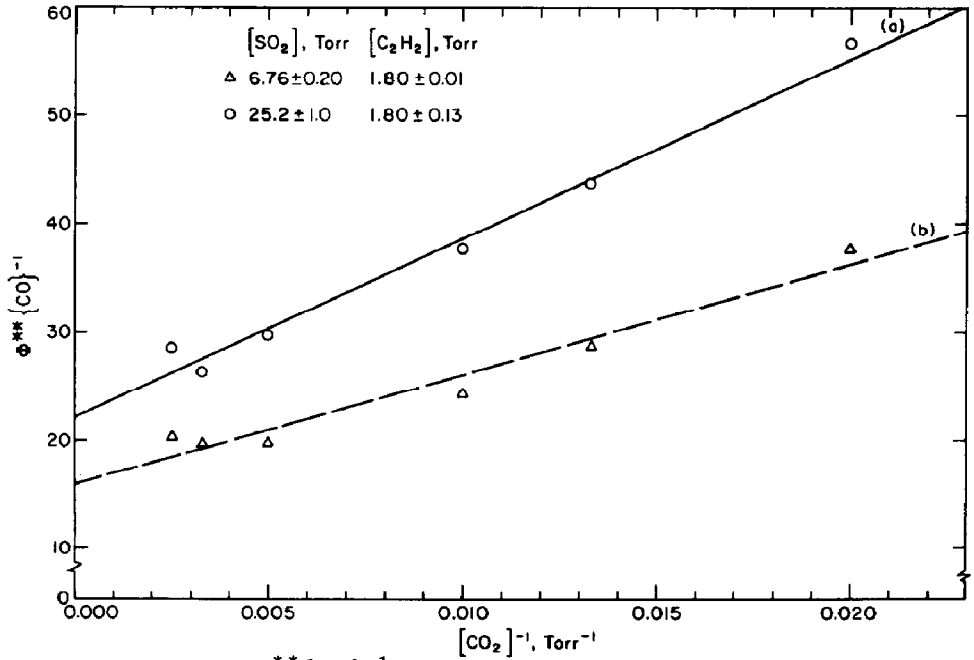


Fig. 8. Plots of $\Phi^{**}\{CO\}^{-1}$ *vs.* $1/[CO_2]$. Table 4 lists the computed points used in the plots.

A few runs were done with water as the quenching gas and only a very small decrease in $\Phi\{CO\}$ was seen. Qualitatively we can say again that as water quenches $SO_2(^3B_1)$, $SO_2^{**}$ is formed from $SO_2^*$ quenching, so that we see no net quenching. If we use the rate constant ratio $k_{8d}/k_{8a} = 1.62$ previously found [3] we may make an estimate of the efficiency with which water causes $SO_2^*$ to cross over to $SO_2^{**}$. Figure 9 shows a plot of $\Phi^{**}\{CO\}^{-1}$ *vs.* $[H_2O]^{-1}$ from which the slope to intercept ratio gives $k_2/k_3$ for water. $\Phi^{**}\{CO\}$ was obtained for the data points of Fig. 4 by taking $\Phi\{CO\}$ for these points and subtracting $\Phi^3\{CO\}$ calculated using $k_{8d}/k_{8a} = 1.62$ [3]. For the two sets of data $[SO_2] = 25.2$ Torr, $[C_2H_2] = 1.79$ Torr; and $[SO_2] = 25.0$ Torr, $[C_2H_2] = 0.34$ Torr; we obtain $k_2/k_3 = 34.6$ and 30.9 Torr respectively. There are very large error limits on this number since a small change in $\Phi\{CO\}$ of ±10% will change the intercept considerably.

Very efficient quenching of $SO_2(^3B_1)$ is observed for NO. It is not necessary to have a high pressure of NO to completely quench $\Phi\{CO\}$, so $\Phi^{**}\{CO\}$ is also zero in this case. Even if NO does interconvert $SO_2^*$ to $SO_2^{**}$, NO is such an efficient quencher of $SO_2^{**}$ that this would not be seen [3]. From the plot of $\Phi\{CO\}^{-1}$ *vs.* [NO] shown in Fig. 4 we obtain $k_{8c}/k_{7a} = 17.6$, which together with $k_{7a}/k_{8a}$ obtained from Fig. 2, curve (a), gives $k_{8c}/k_{8a} = 74.4$. This agrees well with the results of the study at 3130 Å and also with those of Mettee [9] and Stockburger *et al.* [16]. However, it is considerably lower than that of Sidebottom *et al.* [42] and Penzhorn and Gusten [25].

Thus the same basic mechanism that fits the results of the photolysis of $SO_2$ in the presence of acetylene at 3130 Å fits the results of this study.

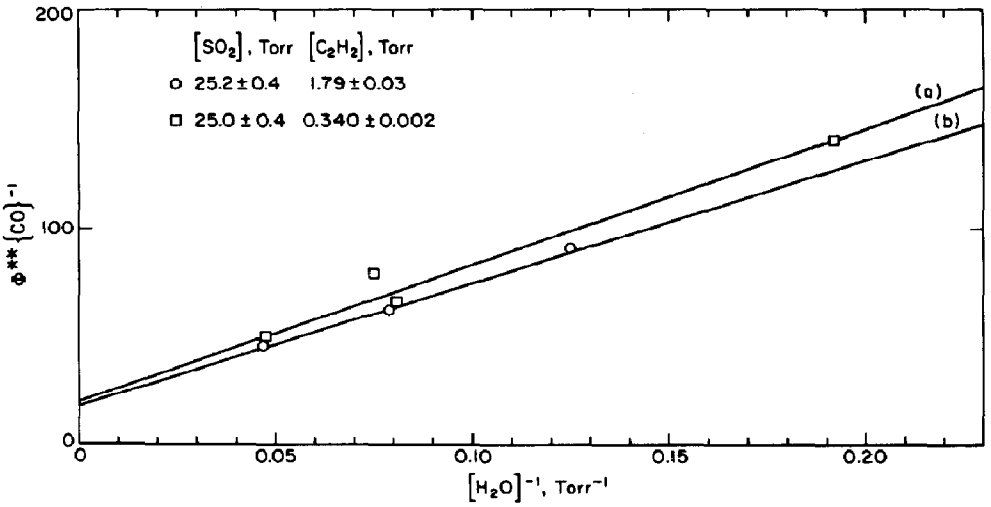


Fig. 9. Plots of $\Phi^{**}\{CO\}^{-1}$ *vs.* $1/[H_2O]$. (a) $[SO_2]$ = 25.2 ± 0.4 Torr; $[C_2H_2]$ = 0.340 ± 0.002 Torr. (b) $[SO_2]$ = 2.50 ± 0.4 Torr, $[C_2H_2]$ = 1.79 ± 0.03 Torr. $\Phi^{**}\{CO\}$ was calculated using the data points of Fig. 5 along with $\Phi^{3}\{CO\}$ calculated using $k_{8d}/k_{8c}$ = 1.62 [3].

In the 3130 Å study, $SO_2^*$ was excited mainly and at high pressures produced $SO_2^{**}$ which accounted for most of the chemistry while $SO_2(^3B_1)$ accounted for the rest. Here $SO_2(^3B_1)$ is the main species formed directly by excitation and accounts for most of the chemistry with a small contribution from $SO_2^{**}$. The summary of all of our rate coefficient data is in Table 1.

Other workers who directly excited the triplet have never needed any other states of $SO_2$ other than $SO_2(^3B_1)$ to account for their results. Our results and conclusions are the same as theirs at low pressures. However, at higher pressures, $SO_2^{**}$ is needed to interpret our results just as seems to be the case when the singlet band is excited at 3130 Å.

## Conclusion

The $SO_2/C_2H_2$ system gives substantial evidence that the emitting states alone cannot explain the photochemistry of $SO_2$. At high pressures additional states become important and the proposed mechanism reproduces the major features of this study satisfactorally. Other mechanisms that have the $SO_2(^3B_1)$ state quenched to a reactive state are unable to fit the results.

## Acknowledgements

We wish to thank Mr. Kenneth Partymiller for helpful discussions, and Dr. Fred Wampler for preprints of his work prior to publication. This work was supported by the Center for Air Environment Studies for which we are grateful (Report No. 427-76).

## References


1 M. Luria, R. G. de Pena, K. J. Olszyna and J. Heicklen, J. Phys. Chem., 78 (1974) 325.
2 M. Luria and J. Heicklen, Can. J. Chem., 52 (1974) 3451.
3 N. A. Kelly, J. F. Meagher and J. Heicklen, J. Photochem., 5 (1976) 355.
4 K. F. Greenough and A. B. F. Duncan, J. Am. Chem. Soc., 83 (1961) 555.
5 R. B. Caton and A. B. F. Duncan, J. Am. Chem. Soc., 90 (1968) 1945.
6 S. J. Strickler and D. B. Howell, J. Chem. Phys., 49 (1968) 1947.
7 H. D. Mettee, J. Chem. Phys., 49 (1968) 1784.
8 H. D. Mettee, J. Am. Chem. Soc., 90 (1968) 2972.
9 H. D. Mettee, J. Phys. Chem., 73 (1969) 1071.
10 T. N. Rao, S. S. Collier and J. G. Calvert, J. Am. Chem. Soc., 91 (1969) 1609.
11 T. N. Rao, S. S. Collier and J. G. Calvert, J. Am. Chem. Soc., 91 (1969) 1616.
12 K. Otsuka and J. G. Calvert, J. Am. Chem. Soc., 93 (1970) 2581.
13 A. Horowitz and J. G. Calvert, Int. J. Chem. Kinet., 4 (1972) 175.
14 A. Horowitz and J. G. Calvert, Int. J. Chem. Kinet., 4 (1972) 191.
15 F. B. Wampler, J. G. Calvert and E. K. Damon, Int. J. Chem. Kinet., 5 (1973) 107.
16 L. Stockburger III, S. Braslavsky and J. Heicklen, J. Photochem., 2 (1973) 15.
17 G. Herzberg, Electronic Spectra of Polyatomic Molecules, Van Nostrand, Princeton, 1960, pp. 511 - 513.
18 P. J. Gardner, Chem. Phys. Lett., 4 (1969) 167.
19 I. H. Hillier and V. R. Saunders, Mol. Phys., 22 (1971) 193.
20 J. V. Brand, W. T. Jones, and C. diLauro, J. Mol. Spectros., 40 (1971) 616.
21 K. L. Demerjian and J. G. Calvert, Int. J. Chem. Kinet., 7 (1975) 45.
22 F. B. Wampler, Int. J. Chem. Kinet., 8 (1976) 519.
23 R. B. Timmons, Photochem. Photobiol., 12 (1970) 219.
24 F. B. Wampler, A. Horowtiz and J. G. Calvert, J. Am. Chem. Soc., 94 (1972) 5523.
25 R. P. Penzhorn and G. H. Gusten, Z. Naturforsch., 27a (1972) 1401.
26 R. A. Cox, J. Photochem., 2 (1973/4) 1.
27 G. E. Jackson and J. G. Calvert, J. Am. Chem. Soc., 93 (1971) 2593.
28 C. C. Badcock, H. W. Sidebottom, J. G. Calvert, G. W. Reinhardt and E. K. Damon, J. Am. Chem. Soc., 93 (1971) 3115.
29 K. L. Demerjian, J. G. Calvert and D. L. Thorsell, Int. J. Chem. Kinet., 6 (1974) 829.
30 F. B. Wampler and J. W. Bottenheim,Int. J. Chem. Kinet., 8 (1976) 585.
31 F. B. Wampler, Int. J. Chem. Kinet., 8 (1976) 687.
32 F. B. Wampler, Int. J. Chem. Kinet., 8 (1976) 511.
33 E. Cehelnik, C. W. Spicer and J. Heicklen, J. Am. Chem. Soc., 93 (1971) 5371.
34 S. Braslavsky and J. Heicklen, J. Am. Chem. Soc., 94 (1972) 4864.
35 E. Cehelnik, J. Heicklen, S. Braslavsky, L. Stockburger III and E. Mathias, J. Photochem., 2 (1973) 31.
36 A. M. Fatta, E. Mathias, J. Heicklen, L. Stockburger III and S. Braslavsky, J. Photochem., 2 (1973) 119.
37 R. D. Penzhorn and W. G. Filby, J. Photochem., 4 (1975) 91.
38 F. B. Wampler, J. G. Calvert and E. K. Damon, Int. J. Chem. Kinetics, 5 (1973) 669.
39 K. Chung, J. G. Calvert and H. W. Bottenheim, Int. J. Chem. Kinetics, 7 (1975) 161.
40 F. C. James, J. A. Kerr and J. P. Simons, Chem. Phys. Lett., 25 (1974) 431.
41 J. G. Calvert and J. N. Pitts, Jr., Photochemistry, John Wiley, New York, 1966, p. 463.
42 H. W. Sidebottom, C. C. Badcock, G. E. Jackson, J. G. Calvert, G. W. Reinhardt and E. K. Damon, Environ. Sci. Technol., 6 (1972) 72.